

Communication

Hydroquinone-Based Anion Receptors for Redox-Switchable Chloride Binding

Daniel A. McNaughton, Xiaochen Fu, William Lewis , Deanna M. D'Alessandro 
and Philip A. Gale * 

School of Chemistry (F11), The University of Sydney, Sydney, NSW 2006, Australia

* Correspondence: philip.gale@sydney.edu.au

Received: 21 June 2019; Accepted: 8 July 2019; Published: 11 July 2019



Abstract: A series of chloride receptors has been synthesized containing an amide hydrogen bonding site and a hydroquinone motif. It was anticipated that oxidation of the hydroquinone unit to quinone would greatly diminish chloride binding affinity of these receptors. A conformational switch is promoted in the quinone form through the formation of an intramolecular hydrogen bond between the amide and the quinone carbonyl, which blocks the amide binding site. The reversibility of this oxidation process highlighted the potential of these systems for use as redox-switchable receptors. ¹H-NMR binding studies confirmed stronger binding capabilities of the hydroquinone form compared to the quinone; however, X-ray crystal structures of the free hydroquinone receptors revealed the presence of an analogous inhibiting intramolecular hydrogen bond in this state of the receptor. Binding studies also revealed interesting and contrasting trends in chloride affinity when comparing the two switch states, which is dictated by a secondary interaction in the binding mode between the amide carbonyl and the hydroquinone/quinone couple. Additionally, the electrochemical properties of the systems have been explored using cyclic voltammetry and it was observed that the reduction potential of the system was directly related to the expected strength of the internal hydrogen bond.

Keywords: anion binding; chloride receptor; switchable system; hydroquinone; redox switch

1. Introduction

Considerable effort has been devoted to the development of sophisticated and functional molecular machine architectures [1–4]. An integral part of this endeavour has focused on constructing simple molecular switches that mimic elegant examples found in nature [5–7] and expanding the scope of their functional remit to new applications [8–12]. This includes the field of anion recognition chemistry, with systems being applied in the detection and extraction of environmentally damaging and biologically important ions [13–16]. Switchable systems associated with anion recognition have focused mainly on anion-mediated events, where a coordination event induces a detectable change in the molecule which can be sensed by a reporter group [17–20]. However, the field is beginning to expand to include systems where the binding itself can be controlled by external stimuli.

We have previously reported examples of pH-dependent anion receptors which promote chloride efflux under acidic conditions [21–23]. Switchable transporters may allow the movement of anions in healthy cells to be regulated, akin to the mechanism found in many transport proteins [7,24], or find use in targeting cancer cells for efflux induced apoptosis [25,26]. Additionally, a small number of compounds has been developed in which anion binding can be controlled by a photophysical input [27,28]. Photoisomerization can be used to alter the shape of the binding cleft, resulting in a difference in binding affinity between the two states [29,30]. The application of switches governed by electrochemical stimuli provides another method through which anions can be bound and released, yet these systems remain underexplored.

The hydroquinone/quinone redox couple is found extensively throughout biology [31,32], and its well-defined electrochemical properties highlighted its potential candidacy for use in a switchable receptor system [33–35]. With this in mind, we designed a simple yet novel receptor scaffold consisting of a hydroquinone motif with an appended benzamide group. It was envisaged that the convergent hydrogen bonds of the amide and one of the hydroquinone OH group could create a chloride recognition site inspired by similar benzenediol receptors [36]. Subsequent oxidation to the corresponding quinone would induce a rotation around the quinone-benzamide bond due to the favorable formation of an intramolecular hydrogen bond, which is demonstrated in Figure 1. The oxidation event removes the OH groups and causes a conformational change in the orientation of the amide NH and would therefore greatly diminish the chloride affinity of the oxidised form of the receptor.

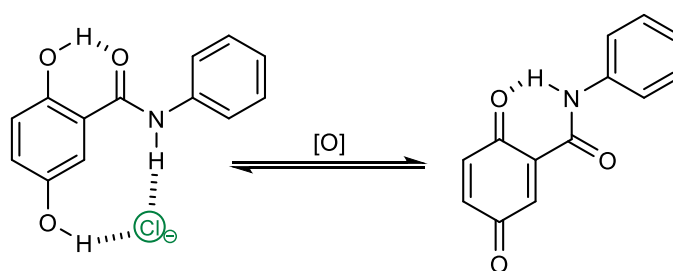


Figure 1. Proposed binding mode of the hydroquinone (left) and proposed intramolecular hydrogen bonded quinone species (right).

A series of hydroquinone-benzamide receptors appended with a variety of electron withdrawing and donating groups was prepared. Subsequently, these molecules were oxidised to afford their quinone forms. Chloride binding affinity has been determined, and the results compared to evaluate the effect of the redox-activated conformational switch on chloride recognition. Additionally, cyclic voltammetry has been used to study the electrochemical properties of the receptors.

2. Results and Discussions

2.1. Synthesis

Hydroquinones **1–4** were prepared following a literature procedure for the parent compound [37], which can be followed in Figure 2. Initially, 2,5-dimethoxybenzoic acid was reacted with oxalyl chloride in dry toluene to afford the acid chloride. Immediate reaction with the respective aniline derivative under basic conditions resulted in the preparation of dimethoxybenzamide compounds **9–12** in yields of between 38–69%. Subsequently, the compounds were reacted with boron tribromide at 0 °C to yield the hydroquinone series. A number of methods were attempted to successfully oxidise the hydroquinones to their quinone forms. Initially, reactions of the hydroquinone compounds with FeCl₃ and cerium ammonium nitrate respectively did not lead to the formation of product. This may be due to the instability of the final product in methanol, which caused conversion back to the hydroquinone species, and separation problems as a consequence of additional products. Incomplete conversion to the quinone product in solution led to the formation of a purple compound, identified as a sandwich quinhydrone-like complex which contains one unit each of hydroquinone and quinone [38].

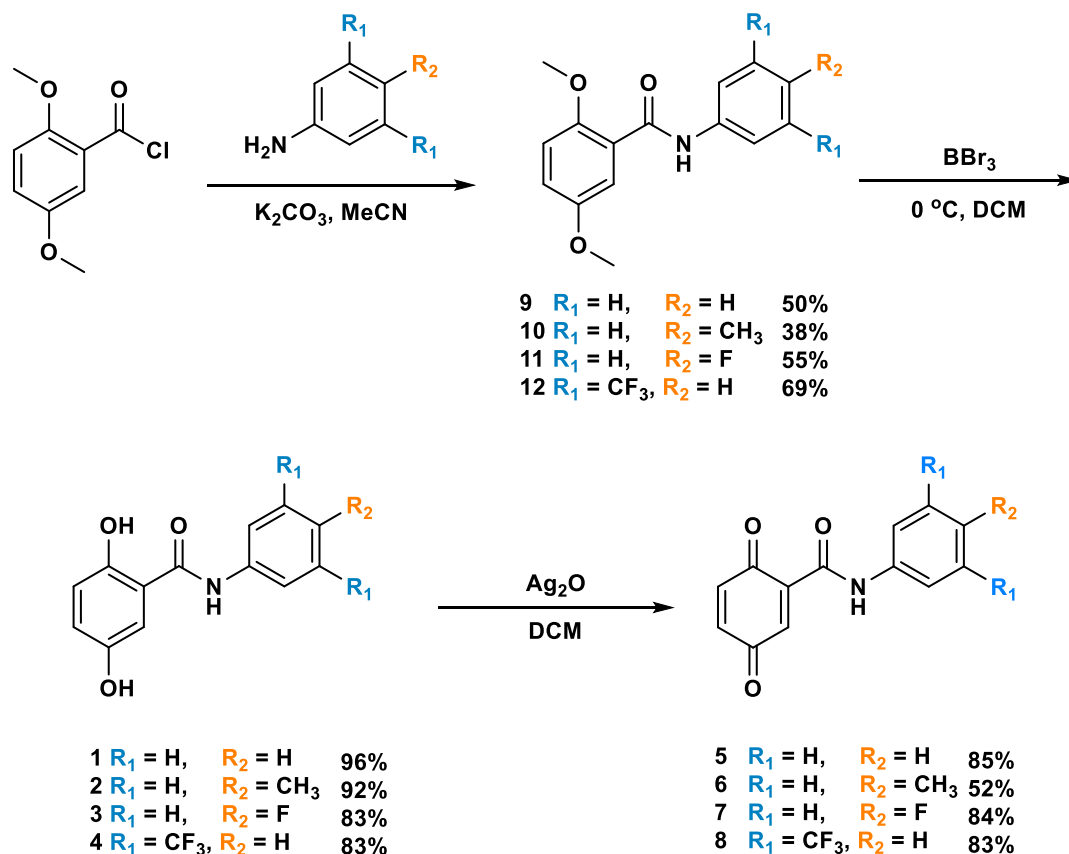


Figure 2. Synthetic procedure for the hydroquinone series and subsequent oxidation to the analogous quinone species.

Conversion was successfully achieved by adding silver oxide to a suspension of the hydroquinone derivatives in dichloromethane [39]. Only the quinone compound enters the solution, meaning the formation of quinhydrone can be avoided. The quinone series was successfully isolated with yields ranging from 52–83%. All new compounds were characterized by ^1H -NMR and ^{13}C $\{^1\text{H}\}$ -NMR. The dimethoxybenzamide and hydroquinone compounds were characterized using Electrospray Ionization (ESI) mass spectrometry, and the quinones using Atmospheric-Pressure Chemical Ionization (APCI) mass spectrometry. Full details and characterization are provided in the Supplementary Materials.

Crystals of Compound 3 were grown by slow evaporation of an acetonitrile solution of the receptor and the structure was elucidated by single crystal X-ray diffraction (CCDC 1919631). The structure (Figure 3a) shows the receptor adopting the expected conformation in the solid state with an intramolecular hydrogen bond between hydroquinone oxygen O17 and amide oxygen O10 (2.52(4) Å). Crystals of Compound 4 were grown in a similar fashion from a saturated acetonitrile solution and the structure was elucidated by single crystal X-ray diffraction (CCDC 1919630). In this case, the compound crystallized as the acetonitrile solvate with the acetonitrile bound via a hydrogen bond to the hydroquinone oxygen (O2 \cdots N2 2.818(9) Å) (Figure 3b). There was an additional intramolecular hydrogen bond between amide N1 and hydroquinone O2 (N1 \cdots O2 2.645(8) Å) stabilizing the solvate in an alternate conformation to that adopted by Compound 3 in the solid state.

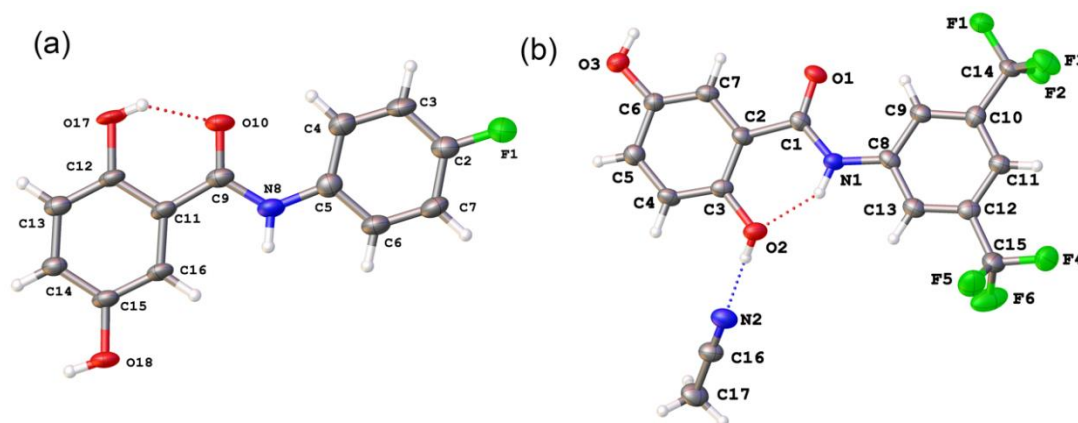


Figure 3. X-ray crystal structures of free receptors 3 (a) and 4 (b).

2.2. Anion Binding Studies

Binding affinities with chloride were determined for Compounds 1–8 using $^1\text{H-NMR}$ spectroscopy titration techniques, with the results displayed in Table 1. Studies for the quinone receptors 5–8 were conducted in pure acetonitrile- d_3 and for the hydroquinones 1–4 in acetonitrile- d_3 /1% DMSO- d_6 to assist with solubility. The amide hydrogen of the quinone species 5–8 was followed and fitted to a 1:1 binding model using Bindfit [40]. For titrations with the hydroquinone species, the change in chemical shift of both the hydroxyl and amide hydrogens were followed where possible. The resultant binding for these compounds proved complex and the data could not be fitted adequately to a 1:1 model. However, fitting to a 2:1 binding model provided a greater than 10 times increase in the quality of fit (cov_{fit} , see supporting information), which is evidence in support of the formation of a 2:1 complex in the presence of small amounts of chloride. It is likely that a 1:1 complex is favored as the concentration of chloride in solution is increased following the equilibrium:



The interaction parameter, α , was calculated for the series 1–4 and was found to have a value of $\alpha > 14$ in all cases. Values of $\alpha > 1$ describe positive cooperative binding [41], and this can be taken as further evidence for the initial favorable formation of a 2:1 complex at low chloride equivalents.

Compound 5 was also titrated with TBACl in acetonitrile- d_3 /1% DMSO- d_6 , the solvent mixture used in the hydroquinone receptor experiments. The more complex 2:1 binding exhibited by receptor 1 means direct comparison is difficult, however both K_{21} and K_{11} for 1 are larger than the association constant for equivalent quinone Compound 5 with chloride. Interestingly, the hydroquinone series do not follow the expected trend where increasing the electron-withdrawing power of the motif appended to the amide increases the binding affinities, because a more polarized N-H bond should result in stronger hydrogen bond formation.

Receptor 4 possesses the most strongly electron-withdrawing substituents and the X-ray crystal structure of the free receptor revealed the presence of a surprising alternate conformation, which can be seen in Figure 3b. In this case, a stronger amide hydrogen bond results in a premature switch in the molecule due to the formation of an intramolecular hydrogen bond between the amide proton and the hydroxyl oxygen. This competing interaction blocks the availability of the binding site, adversely affecting chloride affinity with increasing magnitude for receptors with the highest degree of electron-withdrawing substitution. The chloride binding event reverts the conformation back to the anticipated binding mode, which is evidenced by the downfield shift of both hydroxyl protons during the titration experiments. One hydroxyl group is involved in convergent chloride binding with the amide, while the other shifts due to the formation of another intramolecular hydrogen bond with the

amide carbonyl upon altering conformation. The second hydroxyl peak shift would not be expected to be as significant if due only to inductive effects of chloride binding. This secondary hydrogen bond can also be considered to play a part in the reduction in chloride affinity as stronger electron-withdrawing groups are appended. Removing electron density from the amide carbonyl will deplete the strength of this stabilizing secondary hydrogen bond and hence diminish the favorability of the binding mode.

Table 1. Overview of the 2:1 association constants for the complexation of hydroquinone receptors **1–4** and Cl^- (as TBA salt) in $\text{CD}_3\text{CN}/1\%$ DMSO- d_6 , their interaction parameters (α), and the 1:1 association constants for the complexation of quinone Compounds **5–9** with Cl^- in pure CD_3CN . The 1:1 association constant for **5** and Cl^- in $\text{CD}_3\text{CN}/1\%$ DMSO- d_6 is also reported.

Hydroquinone Receptor	K_{21} ^a	K_{11} ^a	α ^b	Quinone Receptor	K_a ^a
1 ^c	679.5	112.96	24.06	5 ^c	12.57
				5 ^d	11.2
2 ^c	665.6	191.36	13.91	6 ^d	11.39
3 ^c	517.76	30.76	67.33	7 ^d	19.64
4 ^c	336.49	54.44	24.72	8 ^d	67.72

^a All errors < 12%. ^b The interaction parameter (α) is calculated by multiplying K_{21} by 4 and dividing by K_{11} . ^c Titrations performed in $\text{CD}_3\text{CN}/1\%$ DMSO- d_6 at 298K. ^d Titrations performed in pure CD_3CN at 298K.

In comparison, the quinones **5–8** have a stronger chloride affinity with increasingly electron-withdrawing appendages. Repulsion between the quinone carbonyls and the approaching chloride anion inhibits binding, and repulsion is reduced when electron density is pulled away from the quinone system. The anticipated intramolecular hydrogen bond between the amide and hydroquinone carbonyl is still expected to interfere with binding, however in this case the chloride binding event is not enhanced by the formation of a new intramolecular hydrogen bond with the amide carbonyl. Instead, it is hindered by additional repulsion between the amide and quinone carbonyls, which is diminished in the presence of more potent electron-withdrawing groups.

The converse trends in binding strengths between the reduced and oxidised forms of the receptors highlight the importance of the relationship between the hydroquinone/quinone couple and the amide carbonyl in dictating chloride affinity. $^1\text{H-NMR}$ titrations were also performed for the dimethoxybenzamide Compounds **9–12** with TBACl and fitted to a 1:1 binding model. The association constants were all found to be greater than 7 M^{-1} , highlighting the importance of the hydroquinone hydroxyl proton in creating a convergent anion binding site. Full titration data and fitting for these species can be found in the Supplementary Materials. The likely presence of an amide intramolecular hydrogen bond in the lowest energy conformers of both the hydroquinone and quinone forms of the receptors suggest that this singular contribution cannot result in the differences in binding affinity reported. A combination of the relative strengths of this intramolecular bond, the convergent nature of the hydroquinone binding cleft and the influence of the amide carbonyl over the stability of the binding mode all must be factored in when considering the stronger binding exhibited by the hydroquinone species.

2.3. Electrochemical Studies

Cyclic voltammetry (CV) experiments were employed to assess the electrochemical properties and reversibility of the quinone/hydroquinone couples. The compounds were dissolved in a 0.1 M TBAPF₆/CH₃CN solution and the potential was swept at a rate of 100 mVs^{-1} between a range of 800 to -1000 mV . Ferrocene was also added to the solution and used to reference the reduction potentials acquired for each couple, which are displayed in Table 2.

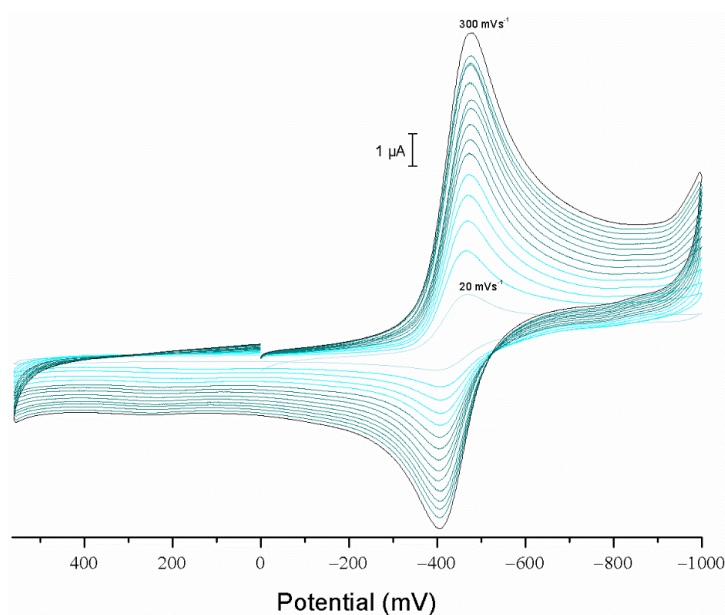
Table 2. Reduction potentials for the quinone species 4–8 obtained using cyclic voltammetry.

Compound	$E_{1/2}$ (mV) ^a
5	−544
6	−552
7	−539
8	−449

^a Reduction potentials obtained at 100 mVs^{-1} over the range 560 to -1000 mV . Potentials were referenced vs a Fc/Fc^+ couple.

The results indicate a direct correlation between the electron-withdrawing power of the functional group and how readily the quinone motif is reduced. The effect of an intramolecular amide hydrogen bond on the quinone reduction potential has been previously reported [34,42], and the trend observed for quinones 5–8 suggests that a similar interaction is in effect. The internal hydrogen bond pulls electron density away from the quinone group, allowing electrons to be accepted more easily by the system. A stronger hydrogen bond will withdraw a greater amount of electron density as evidenced by the reduction potentials of quinones 5 and 8. The presence of strongly withdrawing bis- CF_3 groups in Compound 8 results in an almost 100 mV difference in reduction potential.

The reversibility of the quinone/hydroquinone couple was evaluated by conducting a series of cyclic voltammetry experiments with varying scan rates. The compounds were dissolved in the same solvent mixture used in the previous experiments, and voltammograms were collected between a range of 800 to -1000 mV for a range of scan rates from $20\text{--}300 \text{ mVs}^{-1}$, of which an example can be viewed in Figure 4. The Randles–Sevcik equation states that for an electrochemically reversible process, a plot of I_p (peak current) against $v^{1/2}$ (root of scan rate) should return a linear relationship which passes through the origin [43]. Data were plotted for each of the quinone systems (see Supporting Information) and a linear correlation was observed for quinones 5–7. Compound 8 however did not follow a linear trend and ΔE_p (the separation of the cathodic and anodic peaks) grew larger with increasing scan rate. This indicates that this redox couple is quasireversible, and that the stability of the hydrogen bond may be affecting the kinetics of the electron transfer process.

**Figure 4.** Overlay of cyclic voltammograms of Compound 7 recorded with increasing scan rate from 20 mVs^{-1} to 300 mVs^{-1} . The current response increases with scan rate.

3. Conclusions

We have demonstrated that the hydroquinone/quinone redox couple can be employed in the creation of a redox-switchable chloride receptor. It was discovered that the intramolecular bond initially expected to only be present in the quinone form of the molecule was also present in the hydroquinone receptor, and it is likely this competing interaction led to a reduction in binding capability. Converging trends in binding affinity due to effects dictated by the amide carbonyl resulted in the receptor couples for Compounds **1** and **2** having the greatest difference in binding ability between the two forms of the switch. CV studies highlighted the effect on reduction potential of increasing electron-withdrawing groups, and the results for Compound **8** suggested a loss in reversibility. This can be taken as further evidence of the inhibitory effect of benzamide-appended electron-withdrawing groups on the effectiveness of this class of receptor. Overall, this work has verified the ability of hydroquinone oxidation as a method of reducing anion binding affinity. We are currently exploring the properties of other receptors containing quinoid systems.

Supplementary Materials: The following are available online at <http://www.mdpi.com/2624-8549/1/1/7/s1>.

Author Contributions: Conceptualization P.A.G. and D.A.M.; synthesis, anion binding studies and electrochemical studies D.A.M.; electrochemical studies, X.F. and D.M.D.; crystallography, W.L.; writing—original draft preparation, D.A.M. and P.A.G.; supervision, P.A.G.

Funding: This research was supported by the Australian Research Council (DP180100612) and the University of Sydney.

Conflicts of Interest: The authors declare no conflicts of interest. The funders had no role in the design of the study; in the collection, analyses, or interpretation of data; in the writing of the manuscript, or in the decision to publish the results.

References

1. Balzani, V.; Credi, A.; Raymo, F.M.; Stoddart, J.F. Artificial molecular machines. *Angew. Chem. Int. Ed.* **2000**, *39*, 3348–3391. [[CrossRef](#)]
2. Roke, D.; Wezenberg, S.J.; Feringa, B.L. Molecular rotary motors: Unidirectional motion around double bonds. *Proc. Natl. Acad. Sci. USA* **2018**, *115*, 9423–9431. [[CrossRef](#)] [[PubMed](#)]
3. Altieri, A.; Gatti, F.G.; Kay, E.R.; Leigh, D.A.; Martel, D.; Paolucci, F.; Slawin, A.M.Z.; Wong, J.K.Y. Electrochemically switchable hydrogen-bonded molecular shuttles. *J. Am. Chem. Soc.* **2003**, *125*, 8644–8654. [[CrossRef](#)] [[PubMed](#)]
4. Bruns, C.J.; Stoddart, J.F. Molecular machines muscle up. *Nat. Nanotechnol.* **2012**, *8*, 9. [[CrossRef](#)] [[PubMed](#)]
5. Minamino, T.; Imada, K.; Namba, K. Molecular motors of the bacterial flagella. *Curr. Opin. Struct. Biol.* **2008**, *18*, 693–701. [[CrossRef](#)]
6. Spudich, J.L. Variations on a molecular switch: Transport and sensory signalling by archaeal rhodopsins. *Mol. Microbiol.* **1998**, *28*, 1051–1058. [[CrossRef](#)] [[PubMed](#)]
7. Feng, L.; Campbell, E.B.; Hsiung, Y.; MacKinnon, R. Structure of a Eukaryotic CLC transporter defines an intermediate state in the transport cycle. *Science* **2010**, *330*, 635–641. [[CrossRef](#)] [[PubMed](#)]
8. Feringa, B.L.; Browne, W.R. *Molecular Switches*; John Wiley & Sons: Hoboken, NJ, USA, 2001.
9. Boelke, J.; Hecht, S. Designing molecular photoswitches for soft materials applications. *Adv. Opt. Mater.* **2019**, 1900404. [[CrossRef](#)]
10. Kassem, S.; Lee, A.T.L.; Leigh, D.A.; Markevicius, A.; Solà, J. Pick-up, transport and release of a molecular cargo using a small-molecule robotic arm. *Nat. Chem.* **2015**, *8*, 138. [[CrossRef](#)] [[PubMed](#)]
11. Kistemaker, J.C.M.; Štacko, P.; Roke, D.; Wolters, A.T.; Heideman, G.H.; Chang, M.C.; van der Meulen, P.; Visser, J.; Otten, E.; Feringa, B.L. Third-generation light-driven symmetric molecular motors. *J. Am. Chem. Soc.* **2017**, *139*, 9650–9661. [[CrossRef](#)] [[PubMed](#)]
12. Schmittel, M.; De, S.; Pramanik, S. Reversible ON/OFF nanoswitch for organocatalysis: Mimicking the locking and unlocking operation of CaMKII. *Angew. Chem. Int. Ed.* **2012**, *51*, 3832–3836. [[CrossRef](#)] [[PubMed](#)]
13. Katayev, E.A.; Kolesnikov, G.V.; Sessler, J.L. Molecular recognition of pertechnetate and perrhenate. *Chem. Soc. Rev.* **2009**, *38*, 1572–1586. [[CrossRef](#)] [[PubMed](#)]

14. Moyer, B.A.; Bonnesen, P.V.; Custelcean, R.; Delmau, L.H.; Hay, B.P. Strategies for using host-guest chemistry in the extractive separations of ionic guests. *Kem. Ind.* **2005**, *54*, 65–87. [[CrossRef](#)]
15. Moyer, B.A.; Custelcean, R.; Hay, B.P.; Sessler, J.L.; Bowman-James, K.; Day, V.W.; Kang, S.O. A case for molecular recognition in nuclear separations: Sulfate separation from nuclear wastes. *Inorg. Chem.* **2013**, *52*, 3473–3490. [[CrossRef](#)] [[PubMed](#)]
16. Busschaert, N.; Caltagirone, C.; Van Rossom, W.; Gale, P.A. Applications of supramolecular anion recognition. *Chem. Rev.* **2015**, *115*, 8038–8155. [[CrossRef](#)] [[PubMed](#)]
17. García-Garrido, S.E.; Caltagirone, C.; Light, M.E.; Gale, P.A. Acridinone-based anion receptors and sensors. *Chem. Commun.* **2007**, *14*, 1450–1452. [[CrossRef](#)] [[PubMed](#)]
18. Barendt, T.A.; Rašović, I.; Lebedeva, M.A.; Farrow, G.A.; Auty, A.; Chekulaev, D.; Sazanovich, I.V.; Weinstein, J.A.; Porfyrakis, K.; Beer, P.D. Anion-mediated photophysical behavior in a C60 fullerene [3] rotaxane shuttle. *J. Am. Chem. Soc.* **2018**, *140*, 1924–1936. [[CrossRef](#)]
19. Suk, J.; Naidu, V.R.; Liu, X.; Lah, M.S.; Jeong, K.S. A foldamer-based chiroptical molecular switch that displays complete inversion of the helical sense upon anion binding. *J. Am. Chem. Soc.* **2011**, *133*, 13938–13941. [[CrossRef](#)]
20. Jones, I.M.; Hamilton, A.D. Anion-dependent switching: Dynamically controlling the conformation of hydrogen-bonded Diphenylacetylenes. *Angew. Chem. Int. Ed.* **2011**, *50*, 4597–4600. [[CrossRef](#)]
21. Howe, E.N.W.; Busschaert, N.; Wu, X.; Berry, S.N.; Ho, J.; Light, M.E.; Czech, D.D.; Klein, H.A.; Kitchen, J.A.; Gale, P.A. pH-regulated nonelectrogenic anion transport by Phenylthiosemicarbazones. *J. Am. Chem. Soc.* **2016**, *138*, 8301–8308. [[CrossRef](#)]
22. Busschaert, N.; Elmes, R.B.P.; Czech, D.D.; Wu, X.; Kirby, I.L.; Peck, E.M.; Hendzel, K.D.; Shaw, S.K.; Chan, B.; Smith, B.D.; et al. Thiosquaramides: pH switchable anion transporters. *Chem. Sci.* **2014**, *5*, 3617–3626. [[CrossRef](#)] [[PubMed](#)]
23. Santacroce, P.V.; Davis, J.T.; Light, M.E.; Gale, P.A.; Iglesias-Sánchez, J.C.; Prados, P.; Quesada, R. Conformational control of transmembrane Cl-transport. *J. Am. Chem. Soc.* **2007**, *129*, 1886–1887. [[CrossRef](#)] [[PubMed](#)]
24. Jasti, J.; Furukawa, H.; Gonzales, E.B.; Gouaux, E. Structure of acid-sensing ion channel 1 at 1.9 Å resolution and low pH. *Nature* **2007**, *449*, 316. [[CrossRef](#)] [[PubMed](#)]
25. Sessler, J.L.; Eller, L.R.; Cho, W.S.; Nicolaou, S.; Aguilar, A.; Lee, J.T.; Lynch, V.M.; Magda, D.J. Synthesis, Anion-binding properties, and in vitro anticancer activity of prodigiosin analogues. *Angew. Chem. Int. Ed.* **2005**, *44*, 5989–5992. [[CrossRef](#)] [[PubMed](#)]
26. Ko, S.K.; Kim, S.K.; Share, A.; Lynch, V.M.; Park, J.; Namkung, W.; Van Rossom, W.; Busschaert, N.; Gale, P.A.; Sessler, J.L.; et al. Synthetic ion transporters can induce apoptosis by facilitating chloride anion transport into cells. *Nat. Chem.* **2014**, *6*, 885–892. [[CrossRef](#)]
27. Lee, S.; Flood, A.H. Photoresponsive receptors for binding and releasing anions. *J. Phys. Org. Chem.* **2013**, *26*, 79–86. [[CrossRef](#)]
28. Vlatković, M.; Feringa, B.L.; Wezenberg, S.J. Dynamic inversion of stereoselective phosphate binding to a bisurea receptor controlled by light and heat. *Angew. Chem. Int. Ed.* **2016**, *55*, 1001–1004. [[CrossRef](#)]
29. Li, Z.; Zhang, C.; Ren, Y.; Yin, J.; Liu, S.H. Amide-and urea-functionalized dithienylethene: Synthesis, photochromism, and binding with halide anions. *Org. Lett.* **2011**, *13*, 6022–6025. [[CrossRef](#)]
30. Shimasaki, T.; Kato, S.; Ideta, K.; Goto, K.; Shinmyozu, T. Synthesis and structural and photoswitchable properties of novel chiral host molecules: Axis chiral 2,2'-dihydroxy-1,1'-binaphthyl-appended stiff-stilbene1. *J. Org. Chem.* **2007**, *72*, 1073–1087. [[CrossRef](#)]
31. Nohl, H.; Jordan, W.; Youngman, R.J. Quinones in biology: Functions in electron transfer and oxygen activation. *Adv. Free Radic. Biol. Med.* **1986**, *2*, 211–279. [[CrossRef](#)]
32. Monks, T.J.; Hanzlik, R.P.; Cohen, G.M.; Ross, D.; Graham, D.G. Quinone chemistry and toxicity. *Toxicol. Appl. Pharmacol.* **1992**, *112*, 2–16. [[CrossRef](#)]
33. Rüssel, C.; Janicke, W. Heterogeneous electron exchange of quinones in aprotic solvents: Part III. The second reduction step of p-benzoquinone and its dependence on the supporting electrolyte. *J. Electroanal. Chem. Interfacial Electrochem.* **1986**, *199*, 139–151. [[CrossRef](#)]
34. Eggins, B.R.; Chambers, J.Q. Proton effects in the electrochemistry of the quinone hydroquinone system in aprotic solvents. *J. Electrochem. Soc.* **1970**, *117*, 186–192. [[CrossRef](#)]

35. Walczak, M.M.; Dryer, D.A.; Jacobson, D.D.; Foss, M.G.; Flynn, N.T. pH dependent redox couple: An illustration of the Nernst equation. *J. Chem. Educ.* **1997**, *74*, 1195. [[CrossRef](#)]
36. Winstanley, K.J.; Sayer, A.M.; Smith, D.K. Anion binding by catechols—an NMR, optical and electrochemical study. *Org. Biomol. Chem.* **2006**, *4*, 1760–1767. [[CrossRef](#)] [[PubMed](#)]
37. Wachter, V. Chemical Synthesis of Small Molecule Libraries Around the p-Benzoquinone Scaffold. Ph.D. Thesis, Technical University of Braunschweig, Braunschweig, Germany, 2007.
38. Michaelis, L.; Granick, S. Molecular compounds of the quinhydrone type in solution. *J. Am. Chem. Soc.* **1944**, *66*, 1023–1030. [[CrossRef](#)]
39. Valderrama, J.A.; Zamorano, C.; González, M.F.; Prina, E.; Fournet, A. Studies on quinones. Part 39: Synthesis and leishmanicidal activity of acylchloroquinones and hydroquinones. *Bioorg. Med. Chem.* **2005**, *13*, 4153–4159. [[CrossRef](#)] [[PubMed](#)]
40. Bindfit. Available online: <http://app.supramolecular.org/bindfit/> (accessed on 15 January 2019).
41. Thordarson, P. Determining association constants from titration experiments in supramolecular chemistry. *Chem. Soc. Rev.* **2011**, *40*, 1305–1323. [[CrossRef](#)]
42. Feldman, K.S.; Hester, D.K.; Golbeck, J.H. A relationship between amide hydrogen bond strength and quinone reduction potential: Implications for photosystem I and bacterial reaction center quinone function. *Bioorg. Med. Chem. Lett.* **2007**, *17*, 4891–4894. [[CrossRef](#)]
43. Faulkner, L.R.; Bard, A.J. *Electrochemical Methods: Fundamentals and Applications*; John Wiley and Sons: Hoboken, NJ, USA, 2002.



© 2019 by the authors. Licensee MDPI, Basel, Switzerland. This article is an open access article distributed under the terms and conditions of the Creative Commons Attribution (CC BY) license (<http://creativecommons.org/licenses/by/4.0/>).